

Visualization of grid-generated turbulence in He II using PTV

B Mastracci^{1,2} and W Guo^{1,2}

¹National High Magnetic Field Laboratory, Florida State University, 1800 E Paul Dirac Drive, Tallahassee, FL 32310, USA

²Department of Mechanical Engineering, Florida State University, 2525 Pottsdamer Street, Tallahassee, FL 32310, USA

E-mail: wguo@magnet.fsu.edu

Abstract. Due to its low viscosity, cryogenic He II has potential use for simulating large-scale, high Reynolds number turbulent flow in a compact and efficient apparatus. To realize this potential, the behavior of the fluid in the simplest cases, such as turbulence generated by flow past a mesh grid, must be well understood. We have designed, constructed, and commissioned an apparatus to visualize the evolution of turbulence in the wake of a mesh grid towed through He II. Visualization is accomplished using the particle tracking velocimetry (PTV) technique, where μm -sized tracer particles are introduced to the flow, illuminated with a planar laser sheet, and recorded by a scientific imaging camera; the particles move with the fluid, and tracking their motion with a computer algorithm results in a complete map of the turbulent velocity field in the imaging region. In our experiment, this region is inside a carefully designed He II filled cast acrylic channel measuring approximately 16 x 16 x 330 mm. One of three different grids, which have mesh numbers $M = 3, 3.75, \text{ or } 5 \text{ mm}$, can be attached to the pulling system which moves it through the channel with constant velocity up to 600 mm/s. The consequent motion of the solidified deuterium tracer particles is used to investigate the energy statistics, effective kinematic viscosity, and quantized vortex dynamics in turbulent He II.

1. Introduction and Motivation

Liquid helium-4 undergoes a phase transition when cooled below the λ -transition temperature, $T_\lambda \approx 2.17 \text{ K}$, though it does not solidify (under its own vapor pressure) as most liquids do upon cooling. Instead, ^4He has two liquid phases: the warmer is He I, an ordinary, classical fluid, and the colder is He II. This liquid behaves according to a two fluid model that describes the coexistence of a fully miscible normal fluid component and superfluid component [1]. The normal fluid is considered to be a classical Navier-Stokes fluid, but the superfluid is inviscid and carries no entropy. Furthermore, vorticity in the superfluid is quantized in units of $\kappa = h/m$, where h is Planck's constant and m is the mass of a ^4He atom. Interactions between these so-called quantized vortices and the normal fluid leads to a non-classical force known as mutual friction [2].

A common application for He II is cooling of superconducting systems such as particle accelerators and large superconducting magnets. It is particularly well suited for this purpose because its unique heat transfer mechanism, thermal counterflow, gives it extremely large effective thermal conductivity. In counterflow, the normal fluid carries thermal energy away from a heat source while the superfluid moves toward the source to conserve mass. In the past two decades, considerable research efforts have been focused on understanding this heat transfer mechanism by using direct flow visualization methods [3].



These methods offer high resolution, non-invasive measurements of whole flow fields by means of photography or videography of fluids that have been seeded with small passive tracer particles. However, when traditional visualization techniques, such as particle image velocimetry (PIV) or particle tracking velocimetry (PTV), have been applied to thermal counterflow, the results have been difficult to interpret. In some cases the particles are observed to sporadically change direction, sometimes moving with the expected velocity of the normal fluid and sometimes with the superfluid [4]; in other cases, the particles move uniformly at some speed which is neither the normal fluid nor superfluid velocity [5]. Experimental effort has confirmed that particles can be influenced by both fluid components, and that the motion depends strongly on fluid temperature and magnitude of the heat flux that drives the counterflow [6]. The complexity of particle motion in the two opposing velocity fields makes the suitability of these visualization techniques for thermal counterflow questionable.

Another potential use for He II, which has also been known for decades, is economical reproduction of high Reynolds number flow [7, 8]. The kinematic viscosity of He II, as low as $\nu < 10^{-8}$ m²/s, is lower than that of any other fluid [9]; since the Reynolds number is inversely proportional to kinematic viscosity, $Re = UD/\nu$, where U represents the mean flow velocity and D represents a characteristic length scale, it can be driven to extremely high values even for reasonable container size and flow speed if He II is used as the working fluid. $Re \sim 10^7$ has already been achieved in laboratory apparatus no larger than a couple of meters [10, 11]. By extension, large scale phenomena such as flow around large transportation and defense vessels could be economically generated and studied in the laboratory without the need for large-scale, expensive testing facilities.

Before attempting to launch a high- Re research facility using He II, additional understanding of turbulent flow in this complex two-fluid system is required. Experimental observations suggest that for mechanically generated turbulence in He II, behaviors expected of analogous classical fluid flow can be observed [11, 12, 13, 14, 15], since the two fluids can become coupled together by mutual friction [16]. However, some theoretical and computational efforts do not support this picture [17], or suggest that there are still observable quantities, such as intermittency, that differ between turbulence in He II and classical turbulence [18]. To conclusively characterize the behavior of mechanically generated turbulence in He II, a systematic study of simple, well controlled turbulence that can easily be compared with theoretical models could be of use.

We will discuss our efforts to characterize homogeneous isotropic turbulence (HIT) in He II using direct flow visualization. HIT is the simplest form of turbulence, and has received extensive theoretical and experimental attention in classical fluids research [19]. It is generally accepted that this kind of turbulence is produced when a mesh grid moves through a stationary fluid, so we select this method for generating turbulence in our experiment. Flow visualization using PTV is the preferred diagnostic tool; since coupling of the two fluid components by mutual friction leaves a single velocity field, the ambiguity that plagues visualization of thermal counterflow will be absent from the grid turbulence experiment. We will complement the PTV technique with measurement of second sound attenuation, a widely adopted method for measuring quantized vortex line density in the superfluid component, though this technique will not be discussed in detail. There are two major aspects to conducting this research: first, developing an experimental apparatus that is capable of making the intended measurements, and then analyzing and interpreting the results to address the open questions about turbulence in He II. In Sect. 2 we present the design of a new facility for visualizing grid turbulence in He II (though a more comprehensive discussion of the instrument will be published elsewhere [20]), and in Sect. 3 we explain how the data from our experiment can address some open questions. Sect. 4 is the conclusion.

2. Experimental setup and procedure

Three components are required to perform a flow visualization experiment: tracer particles, which should follow the flow faithfully enough to be considered fluid elements; a light source to illuminate the tracer particles; and a camera to record their motion [21]. In this experiment, a continuous wave blue (473 nm) laser with output power up to 600 mW is shaped into a sheet measuring about 20 mm high by 100 μ m

wide and serves as the light source. The PTV method requires the camera to record a long sequence of images with relatively small separation time, therefore we use a high speed digital video camera with the acquisition rate set for 100 frames per second. The recorded images are processed by an algorithm which is based on a common feature point tracking algorithm [22] that has been modified to suit the He II experiment. This algorithm works by first identifying tracer particles in the images, and then comparing two successive images and linking nearest neighbors into trajectories. The result is an ensemble of spatial and temporal coordinates which describe the trajectories of each particle through the turbulent flow field.

Seeding He II with tracer particles is not a trivial task, and has been a major challenge for He II flow visualization experiments since the earliest velocimetry experiments [23]. A major breakthrough was the use of solidified isotopes of hydrogen, formed by injecting a mixture of hydrogen (or deuterium) and helium gas into liquid He I, and then cooling to the desired He II temperature [24]. However, there are still some drawbacks to this method. It takes time to evaporatively cool through the phase transition from He I to He II, and the particles may not linger in the flow field for long enough to make efficient systematic measurements. There is also a considerable thermal and mechanical disturbance associated with injection of the room temperature gas into liquid helium. More recently, a method was described for introducing solidified particles directly into He II [25], which we have adapted to the grid turbulence experiment. A dilute mixture of deuterium and helium gas is formed using a basic partial pressure blending system, and then the mixed gas is slowly introduced (about $100 \mu\text{g/s}$) to the flow field through a tube that opens just above the laser sheet. Using this method we have been able to reliably produce and image solidified deuterium tracer particles with average size between 4 and $5 \mu\text{m}$.

The visualized flow is generated and contained inside a vertical channel, shown in Fig. 1, which is suspended in an optical access liquid helium cryostat. The channel measures approximately 16 by 16 by 330 mm and is constructed from cast acrylic. This material was selected because it is transparent and can be machined easily; therefore the channel allows optical access, has smooth uniform interior walls which will not snag the grid or induce unwanted turbulent flow, and can be fitted with various instrumentation.

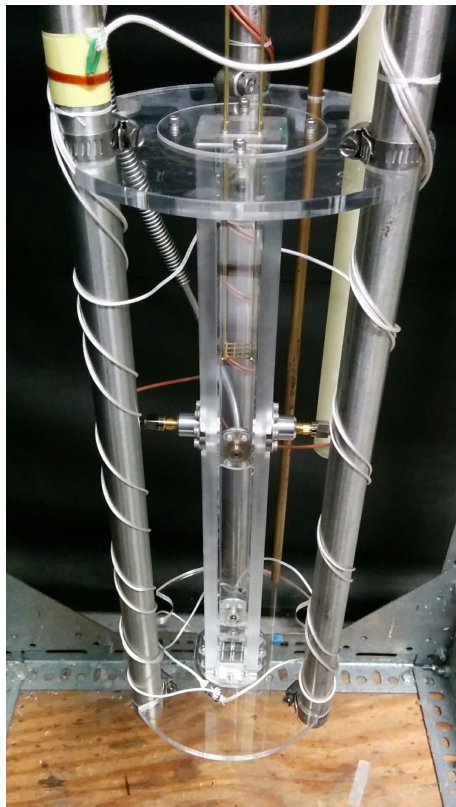


Figure 1. Acrylic flow channel. The mesh grid can be seen inside the channel.

Three grids of similar design but different mesh sizes, shown in Fig. 2, have been produced. The grids occupy the entire cross section of the channel, and the mesh size M , or the sum of one bar width and one hole width, is determined by the number of times the mesh can be repeated in the amount of space available. Mesh sizes of $M = 3$, $M = 3.75$, and $M = 5$ mm, corresponding to a 5 by 5, 4 by 4, and 3 by 3 grid, respectively, were produced from brass sheet stock using a water jet machining center. The shape of the grids, as well as the ratio of bar width to hole width, is based on experience passed on through classical turbulence literature: the ratio of open surface area to solid surface area should be 60% or more, and the grids should be symmetric in the channel walls [26]. We have also considered the effect of heating from the grid dragging against the channel walls, and as a result have extended the four corners slightly beyond the end of the mesh to isolate any contact to the corners of the channel.

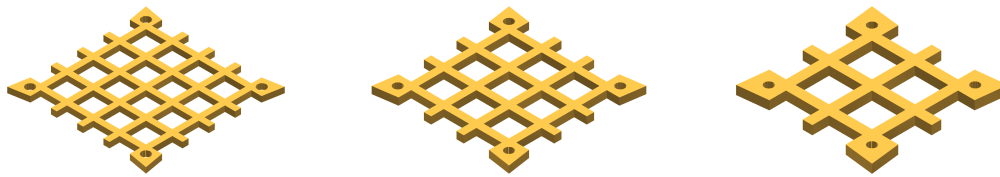


Figure 2. Three mesh grids produced for the experiment. The mesh numbers, from left to right, are $M = 3$ mm, $M = 3.75$ mm, and $M = 5$ mm.

A basic representation of the grid pulling system is shown in Fig. 3. In each corner of the grid, a 1 mm brass wire connects it to a linear drive shaft outside of the channel. The drive shaft passes through the top of the cryostat, where a seal is formed by a metal bellows. This sealing system effectively isolates the low pressure, low temperature environment inside the cryostat from atmospheric conditions throughout

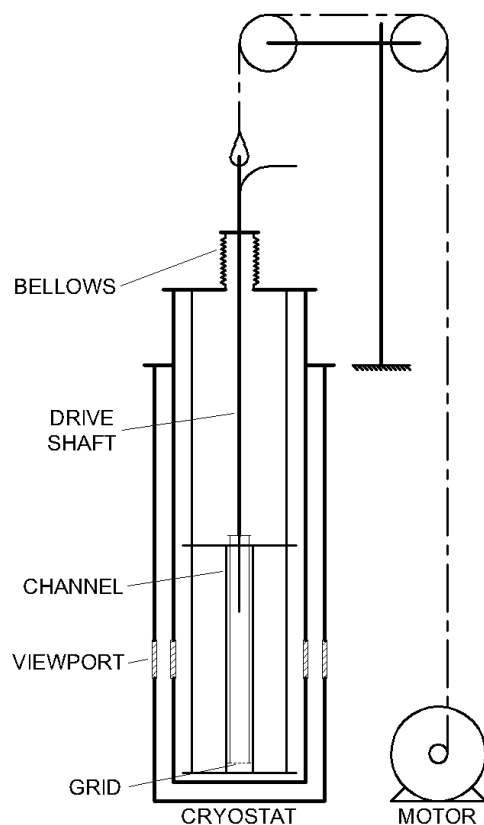


Figure 3. Simple representation of the grid pulling system. The grid and supporting wires are shown inside the acrylic channel. The main linear shaft is pulled by a cable, represented by the broken line, which is routed over a pulley system to an electric motor. The particle delivery tube is inside the main grid shaft, protruding into the channel and exiting from the side of the shaft near the top.

the 300 mm stroke. A cable and pulley system connects the drive shaft to a computer controlled electric stepper motor that generates linear motion by winding the cable around a drum, a simple and intuitive solution that has been used to move a grid through liquid helium in earlier experiments [27]. The system has successfully pulled the grid at speeds between 0.1 and 60 cm/s. Constant velocity is maintained for the middle third of the stroke at 60 cm/s, and for a longer portion of the movement for lower speeds (the grid acceleration is constant). We also note that, since the main grid shaft and tracer particle delivery tube are both required to be above and concentric with the channel, the delivery tube is positioned inside of the drive shaft. In this configuration the particles can be delivered to the optimal location, but the delivery tube moves with the grid assembly and therefore does not obstruct the path of the grid.

3. Data analysis

In preliminary experiments, we have successfully introduced tracer particles, pulled the grid, and visualized the resulting particle motion. An example of the particle tracks extracted from one video is shown in Fig. 4. Each track consists of at least ten spatial and temporal coordinates (\mathbf{x}, t) .

Based on the known position of the particles as they move through the turbulent flow field, the instantaneous velocity at a specific location and time can be easily obtained. If we define one component of the position vector as x , then for a particle appearing in video frame n , the velocity component U in the x direction at time $t = n\Delta t$ can be found from, for example,

$$U = \frac{x_{n+1} - x_n}{\Delta t} \quad (1)$$

The time interval Δt , which represents the amount of time elapsed between the acquisition of successive images, is the same for all of the points along all of the tracks. Since the PTV algorithm requires each track to span at least 10 images, and there are usually many hundreds of tracks extracted from each video, a large ensemble of velocity measurements can be obtained using (1).

One important use of these velocity measurements is an accurate calculation of the effective kinematic viscosity, ν' , for the decay of turbulence in He II. For classical fluids, the kinematic viscosity appears

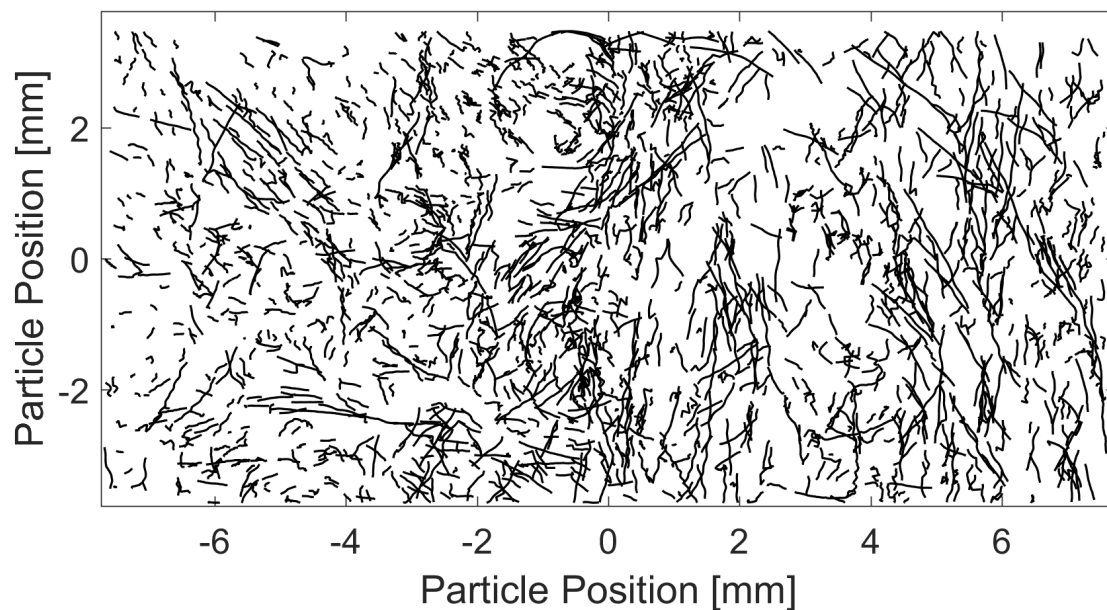


Figure 4. Particle tracks extracted by the PTV algorithm from one video. All of the extracted tracks have been plotted together in the figure; they do not necessarily all appear at the same time in the original video.

as a proportionality constant relating the rate of decay of turbulent kinetic energy, E , to mean square vorticity, ω'^2 [19]:

$$\frac{dE}{dt} = -\nu\omega'^2 \quad (2)$$

The notation ω' denotes the root mean square (rms) vorticity. In He II, the proportionality constant must account for the viscosity of the normal fluid as well as interactions between the two fluid components due to mutual friction, and mean square vorticity is represented by the vortex line density L :

$$\frac{dE}{dt} = -\nu'(\kappa L)^2 \quad (3)$$

The quantity ν' has been measured for He II towed grid turbulence in the past, but it was calculated based on measurements of L and an assumption about dE/dt [28]. A more accurate measurement of ν' can be obtained by measuring both L and E directly. The energy decay rate can be broken into

$$\frac{dE}{dt} = C_1 \frac{dL}{dt} + C_2 u'^2 \quad (4)$$

where C_1 and C_2 are constants and u' represents the rms velocity fluctuation [29]. Measurement of L can be obtained from the traditional second sound method, and u' is easily obtainable from the particle velocity measurements:

$$u' = \sqrt{\frac{1}{N} \sum_i^N (U_i - \bar{U})^2} \quad (5)$$

It is then possible to solve for the effective kinematic viscosity ν' , the only remaining unknown in (3) [29].

Another important measurement of turbulent flow is the energy spectrum, denoted by $E(k)$, which describes the distribution of kinetic energy across turbulent eddies of wave number, or spatial frequency, k . Theories exist for how the energy spectrum should evolve in He II grid turbulence [13, 30], and a reliable experimental measurement is now possible using the velocity measurements from the PTV experiment.

The energy spectrum can be obtained from the Fourier transformation of the Lagrangian velocity autocorrelation coefficient $R_L(\tau)$ [31]:

$$E(k) = 4 \int_0^\infty R_L(\tau) \cos(2\pi k\tau) d\tau \quad (6)$$

The autocorrelation coefficient itself is obtained from the velocity fluctuation data [31]:

$$R_L(\tau) = \frac{\overline{u(t)u(t-\tau)}}{\overline{u'(t)u'(t-\tau)}} \quad (7)$$

The overbar represents an ensemble average, u' again denotes the rms velocity fluctuation, and τ represents a time lag between the two points along the track at which the velocity fluctuation is measured. These quantities come straightforwardly from the particle tracks by use of (1) and (5).

4. Conclusion

Our effort to characterize homogeneous isotropic turbulence in He II is an important step towards taking advantage of the low kinematic viscosity of this fluid for economical high Reynolds number fluid research. This goal is achieved in two steps: first designing an experiment capable of performing such measurements, and then analyzing and interpreting the findings. We have successfully designed and constructed a facility for visualizing, using the PTV method, towed grid turbulence in He II. Suitable tracer particles can be formed in a carefully designed flow channel and their motion in the wake of the towed grid can be clearly observed. Using the resulting particle position and time information, we can resolve the Lagrangian particle velocity and use the data to measure, for example, an effective kinematic viscosity and evolution of the energy spectrum for decaying grid turbulence.

References

- [1] Van Sciver S W 2012 *Helium Cryogenics* New York: Springer
- [2] Vinen W F 1957 *Proc. R. Soc. Lond. A* **242** 493-515
- [3] Guo W, La Mantia M, Lathrop D P and Van Sciver S W 2014 *Proc. Nat. Acad. Sci. USA* **111** 4653-8
- [4] Paoletti M S, Fiorito R B, Sreenivasan K R and Lathrop D P 2008 *J. Phys. Soc. Japan* **77** 111007
- [5] Zhang T and Van Sciver S W 2005 *J. Low Temp. Phys.* **138** 865-70
- [6] Chagovets T V and Van Sciver S W 2011 *Phys. Fluids* **23** 107102
- [7] Skrbek L, Niemela J J and Donnelly R J 1999 *J. Phys.: Condens. Matter* **11** 7761-81
- [8] Sreenivasan K R and Donnelly R J 2001 *Adv. Appl. Mech.* **37** 239-76
- [9] Donnelly R J and Barenghi C F 1998 *J. Phys. Chem. Ref. Data* **27** 1217-74
- [10] Fuzier S, Baudouy B and Van Sciver S W 2001 *Cryogenics* **41** 453-8
- [11] Saint-Michel B *et al* 2014 *Phys. Fluids* **26** 125109
- [12] Maurer J and Tabeling P 1998 *Europhys. Lett.* **43** 29-34
- [13] Stalp S R, Skrbek L and Donnelly R J 1999 *Phys. Rev. Lett.* **82** 4831-4
- [14] Salort J *et al* 2010 *Phys. Fluids* **22** 125102
- [15] Babuin S, Varga E and Skrbek L 2014 *J. Low Temp. Phys.* **175** 324-30
- [16] Vinen W F 2000 *Phys. Rev. B* **61** 1410-20
- [17] Kivotides D 2015 *Europhys. Lett.* **112** 36005
- [18] Boué L, L'vov V, Pomyalov A and Procaccia I 2013 *Phys. Rev. Lett.* **110** 014502
- [19] Hinze J O 1975 *Turbulence* (New York: McGraw-Hill)
- [20] A comprehensive review of the experiment design is being submitted to *Rev. Sci. Instrum.*
- [21] Raffel M, Willert C E and Kompenhans J 1998 *Particle Image Velocimetry: A Practical Guide* (Berlin: Springer-Verlag)
- [22] Sbalzarini I F and Koumoutsakos F 2005 *J. Struct. Bio.* **151** 182-95
- [23] Çelik D, Smith M R and Van Sciver S W 2000 *Adv. Cryo. Eng.* **45** 1175-80
- [24] Bewley G P, Sreenivasan K R and Lathrop D P 2008 *Exp. Fluids* **44** 887-96
- [25] Fonda E, Sreenivasan K R and Lathrop D P 2016 *Rev. Sci. Instrum.* **87** 025106
- [26] Fernando H J S and De Silva P D 1993 *J. Fluid Mech.* **5** 1849-51
- [27] Smith M R, Donnelly R J, Goldenfeld N and Vinen W F 1993 *Phys. Rev. Lett.* **71** 2583-6
- [28] Stalp S R, Niemela J J, Vinen W F and Donnelly R J 2002 *Phys. Fluids* **14** 1377-9
- [29] Gao J, Guo W and Vinen W F 2016 *Phys. Rev. B* **94** 094502
- [30] Skrbek L, Niemela J J and Donnelly R J 2000 *Phys. Rev. Lett.* **85** 2973-6
- [31] Sato Y and Yamamoto K 1987 *J. Fluid Mech.* **175** 183-99

Acknowledgments

This work is supported by U.S. Department of Energy grant DE-FG02-96ER40952. It was conducted at the National High Magnetic Field Laboratory, which is supported by NSF DMR-1157490 and the State of Florida.